Covert sleep-related biological processes are revealed by probabilistic analysis in *Drosophila*

Timothy D. Wiggin[a], Patricia R. Goodwin[a,1], Nathan C. Donelson[b,2], Chang Liu[a,3,4], Kien Trinh[b], Subhabrata Sanyal[b,5], and Leslie C. Griffith[a,6]

[a]Department of Biology, National Center for Behavioral Genomics and Volen Center for Complex Systems, Brandeis University, Waltham, MA 02454-9110; and [b]Neuroscience Discovery, Biogen, Cambridge, MA 02142

Edited by Joseph S. Takahashi, The University of Texas Southwestern Medical Center, Dallas, TX, and approved March 11, 2020 (received for review October 9, 2019)

Sleep pressure and sleep depth are key regulators of wake and sleep. Current methods of measuring these parameters in *Drosophila melanogaster* have low temporal resolution and/or require disrupting sleep. Here we report analysis tools for high-resolution, noninvasive measurement of sleep pressure and depth from movement data. Probability of initiating activity, P(Wake), measures sleep depth while probability of ceasing activity, P(Doze), measures sleep pressure. In vivo and computational analyses show that P(Wake) and P(Doze) are largely independent and control the amount of total sleep. We also develop a Hidden Markov Model that allows visualization of distinct sleep/wake substates. These hidden states have a predictable relationship with P(Doze) and P(Wake), suggesting that the methods capture the same behaviors. Importantly, we demonstrate that both the Doze/Wake probabilities and the sleep/wake substates are tied to specific biological processes. These metrics provide greater mechanistic insight into behavior than measuring the amount of sleep alone.

behavior | Hidden Markov Model | homeostasis | arousal threshold

Sleep is a broadly conserved quiescence behavior that is differentiated from other forms of quiescence (e.g., anesthesia, coma) by its internally driven regulation and fast reversibility (1). In the early 20th century, von Economo argued that control of the transition between sleep and wake was localized to a single "nervous center" (2). In contemporary literature, localization of control over sleep and wake is expressed using the idea of "sleep-promoting" or "wake-promoting" structures or cells. However, far from arising from a single center, there are many interconnected cell groups in the mammalian brain that participate in wake/sleep transitions (3). Even in the fruit fly *Drosophila melanogaster*, which has a much smaller brain than any mammal, the localization of sleep initiation is complex, with dozens of cellular loci that can drive sleep or activity (4). To add further layers of regulation, these neuronal mechanisms are overlaid with a rich pallet of hormonal and metabolic factors that can tip the balance between sleep and wake (5, 6). Currently there are no tools for systematically understanding how the many biological drives toward wake and sleep are integrated in *Drosophila*, especially how they combine with, synergize with, or occlude one another.

The difficulty in integrating these different signals may arise from focusing on a single behavioral measure, the amount of sleep, rather than capturing the underlying biological processes that determine the amount of sleep. Human sleep is regulated both by the intensity of the drive to fall asleep (higher in narcolepsy, lower in insomnia) and the tendency to wake up (higher in insomnia, lower in hypersomnolence and depression) (7, 8). For mammals, the activity of sleep centers in freely behaving animals can be measured using implanted electrodes or noninvasively using electroencephalography (EEG). To capture the underlying neural processes, conditional probability models using neuronal firing or EEG data have been used to model the structure of healthy and disordered sleep in mammals (9–12). Electrophysiological data have also allowed the definition of multiple sleep substates in mammals which reflect higher-order organizational relationships between sleep-regulating nodes.

These types of approaches have not yet been applied to sleep in *Drosophila*. In this paper, we use conditional probability of activity-state switching to measure the biological drives of sleep. We use Hidden Markov Modeling (HMM) as an independent probabilistic metric to validate the transition model and additionally allow us to probe the existence of discrete sleep/wake substates in *Drosophila*.

To investigate the underlying drivers of sleep, we initially consider sleep/wake as a binary choice and define two conditional probabilities: P(Doze), the probability that an active fly will stop moving, and P(Wake), the probability that a stationary

Significance

Reduced sleep duration and disrupted sleep quality are correlated with adverse mental and physical health outcomes. Better tools for measuring the internal drives for sleep and wake in model organisms would facilitate understanding the role of sleep quality in health. We defined two conditional probabilities, P(Wake) and P(Doze), that can be calculated from recordings of *Drosophila* activity without disturbing the animal. We demonstrated that P(Wake) is a measure of sleep depth and that P(Doze) is a measure of sleep pressure. In parallel, we developed an automatic classifier for state-based analysis of *Drosophila* behavior. These analysis tools will improve our understanding of the pharmacology and neuronal regulation of behavioral drives in the *Drosophila* brain.

Author contributions: T.D.W., N.C.D., S.S., and L.C.G. designed research; T.D.W., P.R.G., N.C.D., C.L., and K.T. performed research; T.D.W. analyzed data; and T.D.W. and L.C.G. wrote the paper.

The authors declare no competing interest.

This article is a PNAS Direct Submission.

Data deposition: The MATLAB scripts for analysis of P(Wake)/P(Doze) and for HMM functions have been deposited in GitHub and can be accessed at https://github.com/Griffith-Lab/Fly_Sleep_Probability.

[1]Present address: Department of Medical Writing, Vertex Pharmaceuticals, Boston, MA 02210.

[2]Present address: Division of Lab Operations, LabCentral, Cambridge, MA 02139.

[3]Present address: Shenzhen Key Lab of Neuropsychiatric Modulation, Guangdong Provincial Key Laboratory of Brain Connectome and Behavior, the Brain Cognition and Brain Disease Institute, Shenzhen Institutes of Advanced Technology, Chinese Academy of Sciences, Shenzhen 518053, China.

[4]Present address: Shenzhen-Hong Kong Institute of Brain Science-Shenzhen Fundamental Research Institutions, Shenzhen 518055, China.

[5]Present address: Department of Pharmacology, Calico Labs, South San Francisco, CA 94080.

[6]To whom correspondence may be addressed. Email: griffith@brandeis.edu.

This article contains supporting information online at https://www.pnas.org/lookup/suppl/doi:10.1073/pnas.1917573117/-/DCSupplemental.

First published April 17, 2020.

fly will start moving. Using an in silico model of sleeping flies, we demonstrate that the combination of P(Doze) and P(Wake) is sufficient to explain the total amount of time that flies spend asleep. We experimentally determine that P(Doze) and P(Wake) are measures of sleep pressure and sleep depth, respectively. We find that P(Wake) is strongly influenced by dopamine, the major neurochemical involved in arousal in *Drosophila* (13, 14), and that sleep structure can be regulated by P(Doze) as well as by P(Wake). We find that age-dependent changes in sleep (15, 16) reflect changes in the balance of P(Doze) and P(Wake) and that measurement of transition probabilities reveals aging/sleep interactions.

As a complement and a check on this analysis method, we also developed a Hidden Markov Model for classifying locomotor behavior into four hidden states. This offers the possibility of categorical comparison or real-time perturbation. The HMM hidden states show the predicted correlations with the scalar P(Doze) and P(Wake) conditional probabilities, suggesting that both reflect the same neurological processes. Importantly, the HMM hidden states, like the transition probabilities, are differentially sensitive to experimental manipulation, as would be expected for biologically meaningful sleep/wake substates.

Results

Conditional Wake and Doze Probability Determine *Drosophila* Sleep. Measurement of the amount of sleep in *Drosophila* is based on movement data, typically taken in bins of ≤1 min, where a sleep episode is defined as a certain period of time without movement, usually 5 min (17, 18). The locomotor data are intrinsically binary since only two activity states (active and inactive) can be directly discriminated. Between each individual observation, the fly may choose to either remain in its current activity state or switch. The sequence of activity states reveals not only the amount of time spent in each state, but also the conditional probability of switching states, e.g., from active to inactive. We call the conditional probability $P(\text{Movement}_{\text{time = i}} = 0 \mid \text{Movement}_{\text{time = i-1}} > 0)$ P(Doze) because it is the probability that the fly will switch from the active state to the inactive state. We call the conditional probability $P(\text{Movement}_{\text{time = i}} > 0 \mid \text{Movement}_{\text{time = i-1}} = 0)$ P(Wake) because it is the probability that the fly will switch from the inactive state to the active state (Fig. 1*A*). A detailed explanation of the algorithm for calculating these probabilities and the rationale for using activity/inactivity as the input rather than sleep defined by the 5-min threshold is described in more detail in *Methods* and *SI Appendix*.

These probabilities should change in response to changes in sleep drive and arousal. In order to assess the pattern of activity-state transition probability, we analyzed behavioral data acquired with both the well-characterized *Drosophila* Activity Monitor (DAM) system (*Canton Special* [wild-type, WT] female flies; $n = 60$; Fig. 1) and with the more recently developed FlyBox (WT female flies; $n = 55$; *SI Appendix*, Fig. S1) (19). Both P(Wake) and P(Doze) change across the day, but do not exactly replicate activity, sleep, or one another regardless of the method of data acquisition (Fig. 1 *B* and *C* and *SI Appendix*, Fig. S1*C*). Both P(Wake) and P(Doze) have strong circadian influences, with P(Wake) showing a similarity to locomotor activity. P(Doze) cycles more weakly and circumscribes sleep.

In order to assess the degree of interdependence among these variables quantitatively, we measured the between-animal Pearson correlation of the measures. P(Wake) and total sleep are strongly anticorrelated ($R = -0.92$, $P < 0.0001$), while P(Doze) and total sleep are correlated, but less strongly ($R = 0.26$, $P < 0.0001$). Interestingly, P(Wake) and P(Doze) are only moderately anticorrelated with one another ($R = -0.18$, $P < 0.0001$). These relationships, and the shape of the curves in Fig. 1*B*, suggest that the transition probabilities are not simply each other's inverse, but are instead likely to be driven by distinct sets of biological mechanisms.

The three-way relationship between P(Wake), P(Doze), and sleep (calculated using the 5-min inactivity definition) can be illustrated using a heatmap of total sleep generated at each combination of probabilities (Fig. 1*D*). In order to interrogate the causal relationships between these variables, we used a Markov-chain model to generate in silico behavior. The Markov-chain model is intentionally simplified: it has no circadian rhythms, environmental inputs, etc., making it an ideal environment for determining how changes of only one parameter affect behavior. For the probability bins in which we have in vivo data, there is a surprisingly good match between the in vivo and simplified in silico data (root mean square error = 5.8% Time Asleep, $R = 0.99$, $P < 0.0001$). The lack of unexplained variance in the in vivo data with respect to the in silico data suggests strongly that the combination of P(Wake) and P(Doze) causally determines the amount of total sleep for each individual fly. In addition to the total sleep, sleep episode duration is strongly regulated by P(Wake) (*SI Appendix*, Fig. S2). Previous research has found that each fly has an idiosyncratic preference for a range of behaviors, including total daily sleep (20, 21). We find that P(Wake) and P(Doze) are similarly idiosyncratic, but the population mean is a reasonable estimate of the central tendency of the P(Wake) and P(Doze) distributions for WT flies (*SI Appendix*, Fig. S3).

The daily behavioral cycle of flies can be visualized as trajectories through this probability space (Fig. 1 *F*–*I*). In wild-type animals, the presence of a light cycle generates a double "U"-shaped trajectory (Fig. 1*F*). Removing the light cycle results in a purely linear trajectory through probability space while clock mutant animals maintain the U-shaped trajectory (Fig. 1 *G* and *H*), indicating that the divergence from linearity is caused by light and does not require an intact clock. In the absence of both light cues and a circadian clock, flies simply find their behavioral set point and remain stationary in the probability space (Fig. 1*I*). Given the apparent importance of P(Wake) and P(Doze) in setting the level of total sleep, we sought to relate each to a biological process.

Conditional Wake Probability Is a Measure of Sleep Depth. During sleep, movement and responses to external stimuli are suppressed. The more strongly these behaviors are suppressed, the "deeper" the sleep. Because the likelihood of waking up is logically linked to the depth of sleep, we hypothesized that P(Wake) is a measure of sleep depth. Sleep depth is most commonly measured in flies using arousal threshold (17, 18, 22–25). To examine the relationship between transition probabilities and sensitivity to stimuli, we measured P(Wake), P(Doze), and arousal threshold at two temperatures: a standard temperature (25 °C) and an elevated temperature (29 to 30 °C). Since elevated temperature increases sleep during the day and decreases it at night (26), we hypothesized that sleep depth should also be affected by the change in temperature. As predicted, temperature affects both P(Wake) and P(Doze). P(Wake) is significantly decreased during the daytime ($P < 0.0001$) and elevated during the nighttime ($P < 0.0001$) at 29 °C (Fig. 2*B*). Daytime P(Doze) is significantly elevated by heat ($P < 0.0001$), but nighttime P(Doze) is unchanged ($P = 0.057$).

Because sensitivity to sensory stimuli is also regulated by time of day (24, 27, 28), we measured mechanical arousal threshold with gentle tapping at 3-h intervals across the day using FlyBox (Zeitgeber time [ZT] 1, 4, 7, 10, 13, 16, 19, and 22; $n = 89$ WT female flies). Tapping the flies produced an excess of awakenings compared to chance at time points across the daily cycle at both baseline and high temperatures (Fig. 2*C*). Heat produces significantly anticorrelated effects on P(Wake) and P(Doze) ($R = -0.82$, $P = 0.012$), so the method of partial correlations was

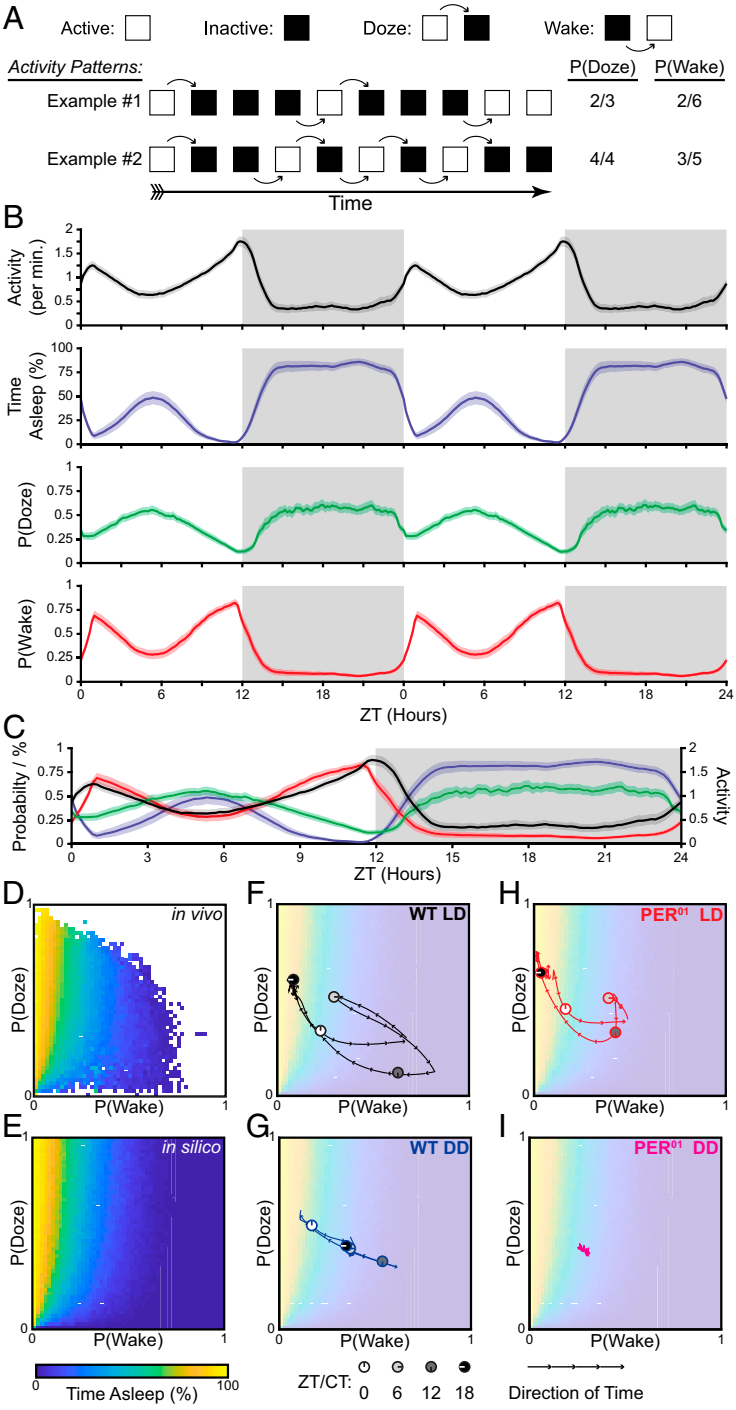

Fig. 1. Conditional wake and doze probability determine *Drosophila* sleep. (*A*) Two exemplar activity patterns (Examples #1 and #2). Open squares: active; black squares: inactive. Transitions between activity states are indicated by curved arrows. Transitions from active to inactive (Doze) are above the blocks; transitions from inactive to active (Wake) are below. Calculation of P(Wake) and P(Doze) are described in *Methods*. (*B*) Double-plotted daily cycles of Activity (black), % Time Asleep (blue), P(Doze) (green), and P(Wake) (red) measured in WT female flies. Solid lines are the population means; tinted bands are the 95% confidence intervals of the means. Individual profiles are the average of 3 d of behavior. Gray area indicates lights-off period. ZT, Zeitgeber time or hours since lights on. (*C*) The same data presented in *B* plotted on a common set of axes. Color coding is the same as in *B*. (*D* and *E*) Heatmaps of in vivo (*D*) and in silico (*E*) sleep properties. The behavior of each in vivo fly was split into 90-min time intervals, and the P(Wake), P(Doze), and total sleep for that interval were calculated. Each 90-min behavioral sample was assigned to one of 51 bins from 0 to 1 based upon its respective P(Doze) and P(Wake). The mean value of total sleep was calculated for the samples in each bin, and the bin was assigned a color according to the legend (below). Coordinates without any biological samples are displayed as white. (*E*) For each P(Doze) and P(Wake) bin, 64 in silico flies were simulated. The mean total sleep in these simulations is displayed using the same color map as the in vivo data. The in silico behavior is subject to the same definition of sleep as in vivo data (5 min of inactivity), which results in the heatmap not having a linear/diagonal gradient. (*F–I*) Plots of the mean trajectory of flies through the P(Wake) vs. P(Doze) probability space across their daily rhythm superimposed on the in silico-predicted total sleep at each point. The direction of time is indicated by arrowheads. Important circadian times are indicated by small clock faces (see key below). Genotype and environmental conditions are indicated in the corner of each plot. PER^{01}: *period* point mutation; LD: 12:12 light:dark cycle; DD: constant darkness.

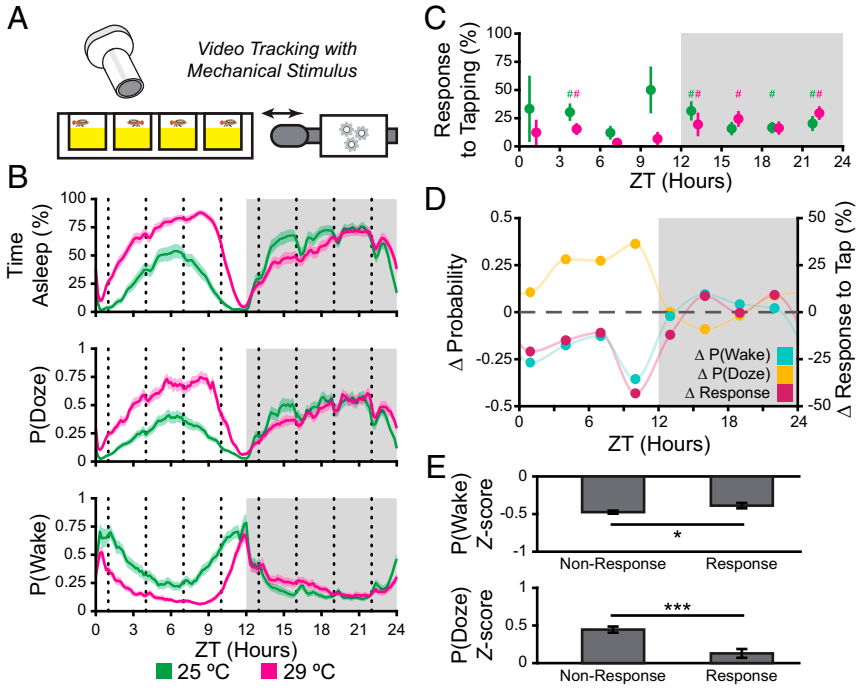

Fig. 2. Conditional wake probability is a measure of sleep depth. (*A*–*E*) Results of a mechanical arousal threshold experiment. (*A*) Schematic of experimental setup. Fly locomotion in a 96-well plate was monitored using a FlyBox. At 3-h intervals starting at ZT 1, an electromagnetic solenoid was used to tap the side of the plate. (*B*) Circadian profiles of % Time Asleep, P(Doze), and P(Wake). Solid lines are the population means; tinded bands are the 95% confidence intervals. Behavior was measured at 25 °C (green) and 29 °C (magenta). Tapping times are indicated by dashed vertical lines. Gray area indicates lights-off period. (*C*) Response to tapping was measured as the increase in arousal probability following a tap. The percentage (%) responding is plotted at 25 °C (green) and 29 °C (magenta). The symbol "#" indicates a response greater than chance ($P < 0.05$) as measured by Fisher's exact test with the Holm's step-down correction for multiple testing. (*D*) The effect of temperature on P(Wake) (cyan), P(Doze) (yellow), and response to tapping (pink) at each time (ZT). (*E*) The P(Wake) and P(Doze) of each time point was normalized by converting it to a *z*-score. The behavior of each fly following each tap was classified as a nonresponse (no activity 1 min after tap) or as a response. The mean *z*-score across all time points for responders and nonresponders is plotted. Error bars are SEM. $*P < 0.05$; $***P < 0.0005$.

used to determine their independent associations with arousal threshold. The effect of heat on the response to tapping across time points is significantly correlated with the effect of heat on P(Wake) ($R = 0.84$, $P = 0.016$) but not the effect of heat on P(Doze) ($P = 0.77$; Fig. 2*D*). When we normalized P(Wake) and P(Doze) between time points, individual flies that responded to the tap had a significantly higher P(Wake) and significantly lower P(Doze) than the nonresponsive flies ($P = 0.024$ and $P < 0.0001$, respectively; Fig. 2*E*). We conclude from this experiment that P(Wake) and arousal threshold are regulated identically by heat, in line with our prediction. As an independent probe of the association of transition probabilities with sleep depth, we measured light-mediated arousal threshold with flashes of red light across the day using the DAM system ($n = 117$ WT female flies; *SI Appendix*, Fig. S4). The effect of heat on light arousal is highly correlated with the effect of heat on P(Wake) ($R = 0.92$, $P = 0.02$) but not well-correlated with the effect of heat on P(Doze) ($P = 0.06$). Within each time point, individual flies that responded to the light had a significantly higher P(Wake) than the nonresponsive flies ($P < 0.0001$), but there was no difference in P(Doze) ($P = 0.15$).

In summary, the effect of heat on arousal threshold is tightly coupled with the effect of heat on P(Wake) regardless of the sensory modality or monitoring system used. Coupling between mechanical arousal threshold and P(Doze) was seen only when normalizing P(Doze) between time points in the comparison of responding vs. nonresponding individuals (Fig. 2*E*). We posit that the association in this experiment is due to the latent correlation between P(Wake) and P(Doze) noted previously and does not reflect a major role for P(Doze) in regulating arousal threshold. This latent correlation is removed by the partial linear correlation method (used to analyze data in Fig. 2*D* where there is no P(Doze)/arousal threshold association) but is not removed in the comparison of responders and nonresponders in Fig. 2*E*. We therefore conclude that P(Wake) and arousal threshold, but not P(Doze), measure the same underlying biological process, namely, sleep depth.

Conditional Doze Probability Is a Measure of Sleep Pressure. Sleep deprivation in flies, like in other animals, leads to increased subsequent sleep (17, 18). A common model for the generation of increased sleep after release from sleep deprivation posits that there is an increase in sleep "pressure" which increases sleep drive (29, 30). Because sleep drive increases the tendency to fall asleep, we hypothesized that P(Doze) is related to sleep pressure.

To increase sleep pressure and examine its relationship to P(Doze), we performed a daytime (ZT 0 to 12) sleep deprivation (SD) experiment (WT female flies; $n = 116$ SD, 118 controls; Fig. 3*A*). Because the expression of recovery sleep is regulated by time of day (31), we hypothesized that the sleep homeostat would maintain a "memory trace" of sleep debt during times of day when recovery sleep is not normally expressed. Flies acquire sleep debt during shaking, P(Wake) is up-regulated, and P(Doze) is down-regulated (Fig. 3 *B* and *C*). Following release from sleep deprivation at ZT 12, P(Doze) is up-regulated, but sleep debt is only minimally discharged during the night, with most of the recovery sleep occurring during the next light period (Fig. 3*B*). P(Doze) remains elevated for 24 h until sleep debt is

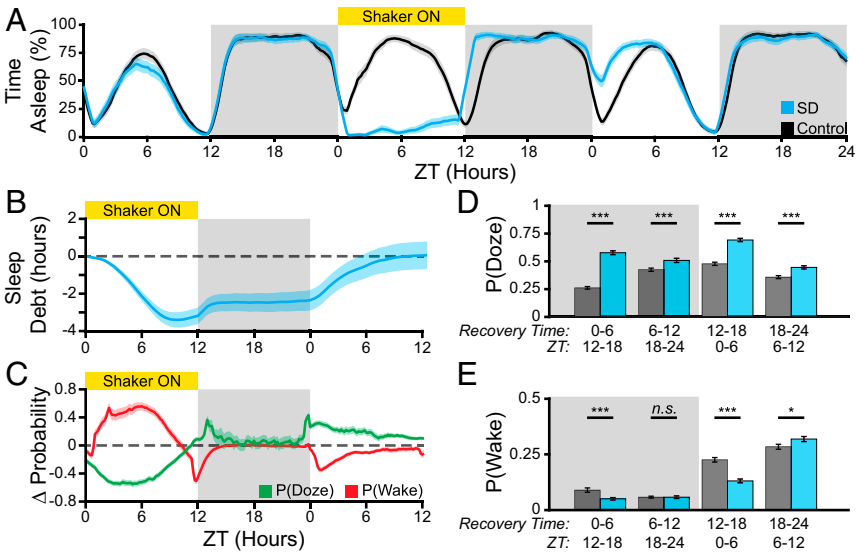

Fig. 3. Conditional doze probability is a measure of sleep pressure. Results of a daytime sleep deprivation experiment. (*A*) The percentage (%) of Time Asleep of shaken (cyan) and unshaken control (gray) flies over 3 d, including 1 d of sleep deprivation. (*B*) Sleep debt accumulated during daytime sleep deprivation and recovered following release from deprivation. (*C*) Change in P(Doze) (green) and P(Wake) (red) during sleep deprivation and following release from deprivation. (*D* and *E*) Comparison of P(Doze) (*D*) and P(Wake) (*E*) between shaken (cyan) and control (gray) flies following release from sleep deprivation. Error bars are SEM. *n.s.*, no significant difference; **P* < 0.05; ****P* < 0.0005.

fully discharged ($P < 0.0005$; Fig. 3*D*). In contrast, P(Wake) is significantly suppressed only during the times of day when recovery sleep is actually being performed, i.e., in the early evening (ZT 12 to 18; $P = 0.0005$) and in the morning presiesta (ZT 0 to 6; $P < 0.0001$; Fig. 3*E*). We also performed nighttime SD by shaking flies between ZT 12 and 24 (WT female flies; $n = 120$ SD, 117 controls; *SI Appendix*, Fig. S5). As expected, sleep debt was discharged immediately following release from nighttime SD, so it did not allow either P(Wake) or P(Doze) to be excluded as a measure of sleep pressure.

These experiments demonstrate that P(Doze) has properties consistent with a measure of sleep pressure: it is elevated by sleep deprivation and returns to baseline only after sleep debt is discharged. In contrast, suppression of P(Wake) is necessary for the expression of rebound sleep but does not have the same memory trace properties as P(Doze). Consistent with P(Wake) driving the expression of rebound sleep, the total amount of rebound is more strongly correlated with change in P(Wake) ($R = -0.97$, $P < 0.0001$) than change in P(Doze) ($R = 0.19$, $P = 0.06$), and the effect size of the change in P(Wake) is larger than

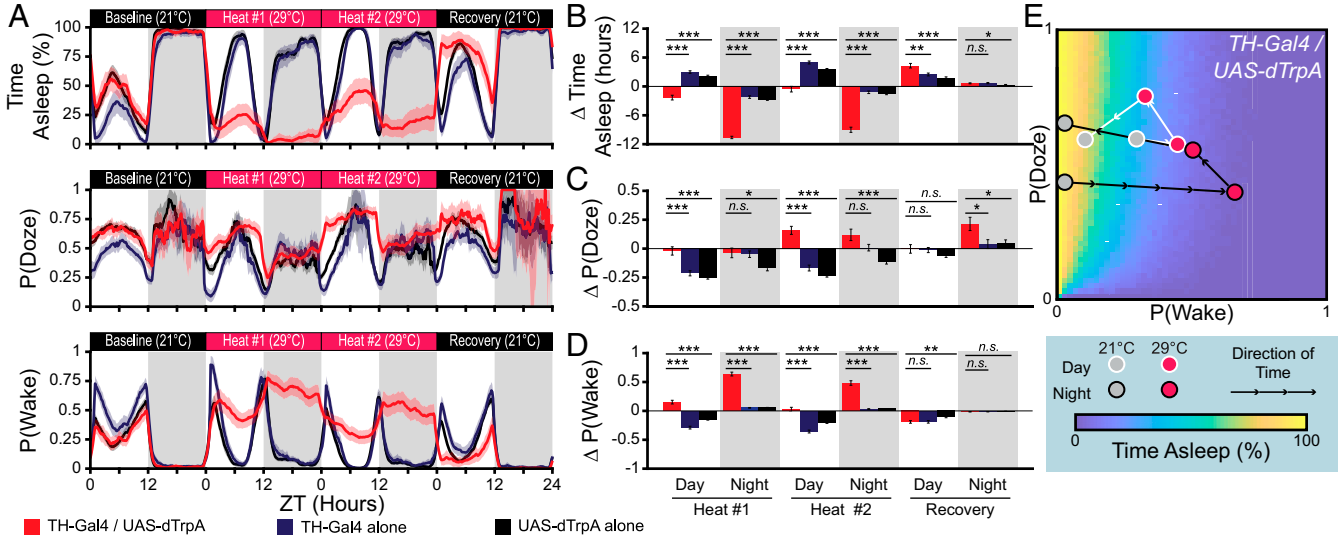

Fig. 4. Dopaminergic tone regulates sleep depth. (*A*) Sleep, P(Doze), and P(Wake) during the thermogenetic activation of dopamine neurons. The experimental flies (red) were compared with control flies carrying only the driver *(TH-Gal4* alone, blue) or only the actuator *(UAS-dTrpA,* black). (*B–D*) Comparison of the heat-induced change in total sleep (*B*), P(Doze) (*C*), and P(Wake) (*D*) between experimental flies and control flies. (*E*) The population mean of the *TH-Gal4/UAS-dTrpA* experimental group during the thermogenetic activation experiment is overlaid on the in silico-predicted sleep heatmap. Arrows indicate the direction of time; gray circles: 21 °C; red circles: 29 °C. Circles with white borders are daytime values, circles with black borders are nighttime values. Error bars are SEM. *n.s.*, no significant difference; **P* < 0.05; ***P* < 0.005, ****P* < 0.0005.

the effect size of P(Doze) (Cohen's d = −1.46 and 0.81, respectively) (32).

One implication of this result is that the magnitude of rebound sleep is a flawed measure of sleep homeostasis, consistent with recent reports (21). Interestingly, P(Doze) also appears to be regulated by "wake pressure" in addition to sleep pressure. This is most obvious during the shaking period, when P(Doze) is down-regulated because disruptive mechanosensory inputs provide an environmentally driven wake pressure (Fig. 3*C*). There are also likely effects of internally generated wake pressure. These can also be inferred from the decrease in P(Doze) during the anticipatory evening activity peak before ZT 12 in unperturbed flies (Fig. 1*B*). We conclude that P(Doze) is a measure of sleep pressure, with the caveat that strongly wake-maintaining processes (sensory, circadian, or otherwise) can mask our ability to detect sleep pressure via behavioral outputs.

Dopaminergic Tone Regulates Sleep Depth. Sleep is regulated by a multitude of molecular processes, and many null and hypomorphic mutations disrupt sleep in flies (33). Dopamine in particular has a role in regulating sleep quantity by increasing arousal (13, 14), and acute activation of dopaminergic neurons has been shown to decrease total sleep (16, 34–36). In order to validate the proposed biological significance of P(Wake) and P(Doze) described above, we measured the effect of manipulating dopaminergic tone on activity-state transition probability by performing a 2-d thermogenetic activation (37) of *TH-Gal4*–positive dopamine neurons (Fig. 4*A*). In order to separate the effect of dopamine neuron activation from the direct effect of temperature on sleep (Fig. 2), we compared the effect of our heat manipulation on the experimental line (*TH-Gal4*/*UAS-dTrpA* female flies, $n = 31$) with the effect on parental strain controls (*TH-Gal4*/+ female flies, $n = 31$; *UAS-dTrpA*/+ female flies, $n = 61$). An effect on behavior was attributed to dopamine neuron activation only when the experimental line was significantly different from both control genotypes.

As has been previously shown, activating dopamine neurons significantly reduces total sleep throughout the activation period ($P < 0.0001$; Fig. 4*B*). This is accompanied by a very substantial increase in P(Wake) throughout the activation period ($P < 0.0001$; Fig. 4*D*) with only a modest daytime increase in P(Doze) ($P < 0.0001$; Fig. 4*C*). Sleep episode duration is also significantly reduced during the daytime by dopamine neuron activation (*SI Appendix*, Fig. S6). Following the cessation of activation, the experimental line had significantly increased sleep ($P < 0.0018$), but P(Wake) and P(Doze) were not significantly altered compared to controls. Close examination of the behavioral traces (Fig. 4*A*) suggests that there may be transient differences in P(Wake) and P(Doze) immediately after temperature is restored to baseline, but the change is not maintained long enough to reach statistical significance when averaged across the entire lights-on period. Because temperature has a strong effect on sleep independent of dopaminergic activation, we also investigated chronic genetic perturbations of the dopamine system (*SI Appendix*, Fig. S7). Both mutants have increased P(Wake) but have opposite changes in P(Doze) (*SI Appendix*, Fig. S7 *C* and *D*).

The overall effect of dopamine on P(Doze) is variable and contingent: only some genetic contexts, time windows, and environmental conditions produce perturbations. On the other hand, acute activation of dopamine neurons and chronic increases of dopaminergic tone increase P(Wake) across all experimental conditions, supporting the idea that P(Wake) is a measure of sleep depth. The conditional changes in P(Doze) may reflect indirect processes or network level linkage.

High-Sucrose Diet Promotes Sleep Consolidation by Decreasing Sleep Pressure. Both sleep deprivation and manipulations of the dopamine system produce dramatic changes in total sleep (Figs. 3 and 4). In order to test the relationship of P(Wake) and P(Doze) to sleep structure, we measured behavior of WT flies fed either a low (2.5%) or a high (30%) concentration of sucrose, a manipulation which has been shown to regulate sleep fragmentation independent of total sleep (23). In agreement with these findings, we do not observe dramatic changes in the daily sleep pattern between low- and high-sucrose diet (WT female flies; $n = 90$ low sucrose, 94 high sucrose; Fig. 5*A*). The effects on the amount of sleep are modest: no effect of diet on daytime sleep and a small increase in nighttime sleep ($P = 0.0001$; Fig. 5*B*).

There is, however, a large decrease in the number of sleep episodes both during the day and at night in the high-sucrose group ($P < 0.0001$; Fig. 5*C*). Interestingly, we find that P(Wake) is unaffected by diet during the daytime but significantly decreased at night ($P < 0.0001$; Fig. 5*D*), in concordance with the effect of sucrose on total sleep. P(Doze) is decreased by high sucrose during both daytime and nighttime, mirroring the effect of sucrose on sleep structure ($P < 0.009$; Fig. 5*E*). In sum, the effect of sucrose on P(Wake) is variable and contingent—it is

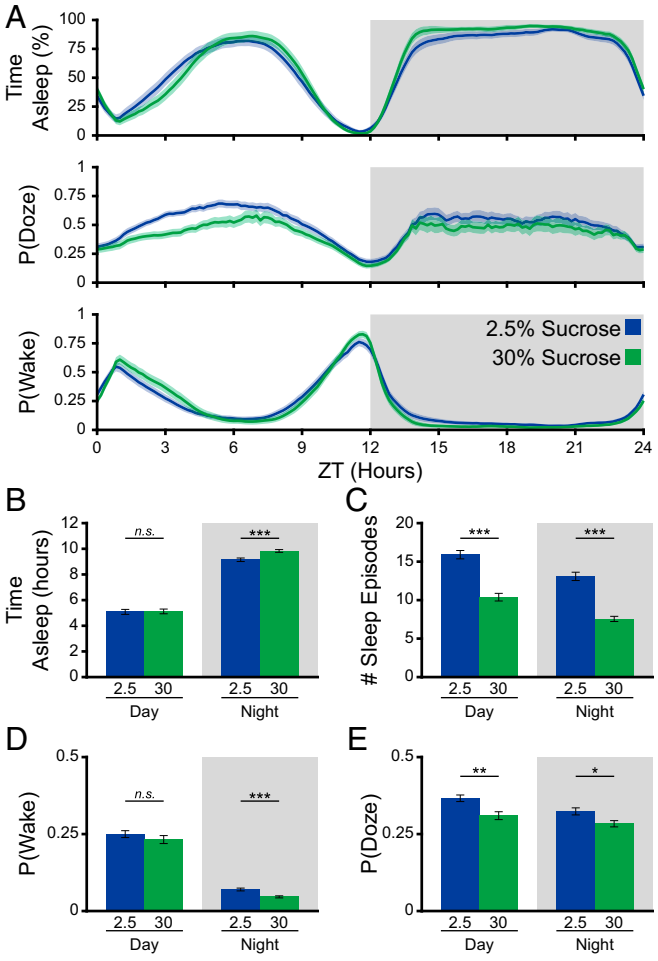

Fig. 5. High-sucrose diet promotes sleep consolidation by decreasing sleep pressure. (*A*) Daily cycle of percentage (%) Time Asleep, P(Doze), and P(Wake) for wild-type (CS) flies fed either a low-sucrose (2.5% sucrose in agar, blue) or a high-sucrose (30% sucrose in agar, green) diet. (*B*–*E*) Comparison of low- and high-sucrose diet time asleep (*B*), number (#) of sleep episodes (*C*), P(Wake) (*D*), and P(Doze) (*E*) during daytime and nighttime. *n.s.*, no significant difference; $*P < 0.05$, $**P < 0.005$, $***P < 0.0005$.

perturbed only at night—while the effect of sucrose on P(Doze) and sleep structure is consistent.

This was an unexpected finding because the initial report of a sucrose effect on sleep structure attributed the effect to sleep depth (23). This discrepancy is likely due to this prior study measuring sleep depth (via arousal threshold) only at night, a time at which we also find a small difference in P(Wake) (Fig. 5*D*). With our improved analysis tools, sleep depth and pressure can be estimated throughout the day, allowing us to separate the different dimensions of diet/environmental interactions and conclude that the change in sleep structure is more likely due to P(Doze), a surprising and interesting finding since fragmentation is usually thought to be due to changes in arousal (*Discussion*).

Changes in Sleep with Age Are due to Both Sleep Pressure and Depth. To test the utility of our analysis tools in understanding a complex, longitudinal biological process, we compared the behavior of flies of different ages. The total amount and structure of sleep produced by an individual is strongly regulated by age in many animals, including flies (15, 16). Sleep was measured in cohorts of WT flies during weeks 1, 3, 5, and 7/8 post eclosion (n = 48, 30, 30, and 39, respectively; weeks 7 and 8 were combined due to a low rate of survival to this age). In agreement with prior results, the daily profile of sleep is altered in aged flies, most dramatically during the day (Fig. 6*A*). In these cohorts of flies, old flies slept significantly longer than young flies ($P < 0.0002$; Fig. 6*B*). Perhaps surprisingly, given our results with groups of young flies (Figs. 1–3) where the amount of sleep was determined largely by changes in P(Wake), nighttime P(Wake) does not vary significantly as flies age, and daytime P(Wake) is significantly decreased only in the oldest group of flies ($P < 0.0001$; Fig. 6*E*). In contrast, P(Doze) increases with age during both the day and the night ($P < 0.0001$; Fig. 6*D*).

Plotting the changes in P(Wake) and P(Doze) as a trajectory through probability space allows us to assess how aging-related changes in behavioral transition probability are related to total sleep (Fig. 6*F*). Nighttime behavior follows a linear path, the extent of which falls within a rather uniformly high-sleep area of the probability space, consistent with the relatively modest changes in sleep quantity at night (Fig. 6 *A* and *B*). Daytime behavior follows a more complex path that moves from a low-sleep area of the space toward a high-sleep area. In this aging dataset, changes in behavior are generated by alterations in both P(Wake) and P(Doze). The effect of aging on nighttime P(Doze) is much stronger than the effect on the amount of sleep. Our method of analysis reveals an "invisible" sleep/aging interaction that would not be apparent with currently used sleep metrics. Determining the biological basis of this shift in transition probability will provide insight into the aging process.

A Four-State Hidden Markov Model of Sleep Pressure and Depth. P(Doze) and P(Wake) provide a continuous integrated view of the activity of all potential wake- or sleep-promoting systems. But sleep-regulating centers likely do not operate completely independently: electrophysiological data in mammals has shown that coordination of activity in particular sleep circuits can produce sleep substates with distinct properties. Human sleep is composed of Rapid-Eye Movement (REM) sleep and either three or four non-REM stages (38, 39). Rodent sleep is usually quantified more coarsely using only two substates (REM and non-REM) (40), but the existence of additional substates has been proposed (41). Distinct sleep stages have been proposed in flies (24), but there has not been a method for detecting these stages in free-behaving animals. Building upon our validation of P(Wake) and P(Doze) as markers of sleep depth and pressure, we developed an HMM that classifies fly behavior into one of four hidden states (Fig. 7).

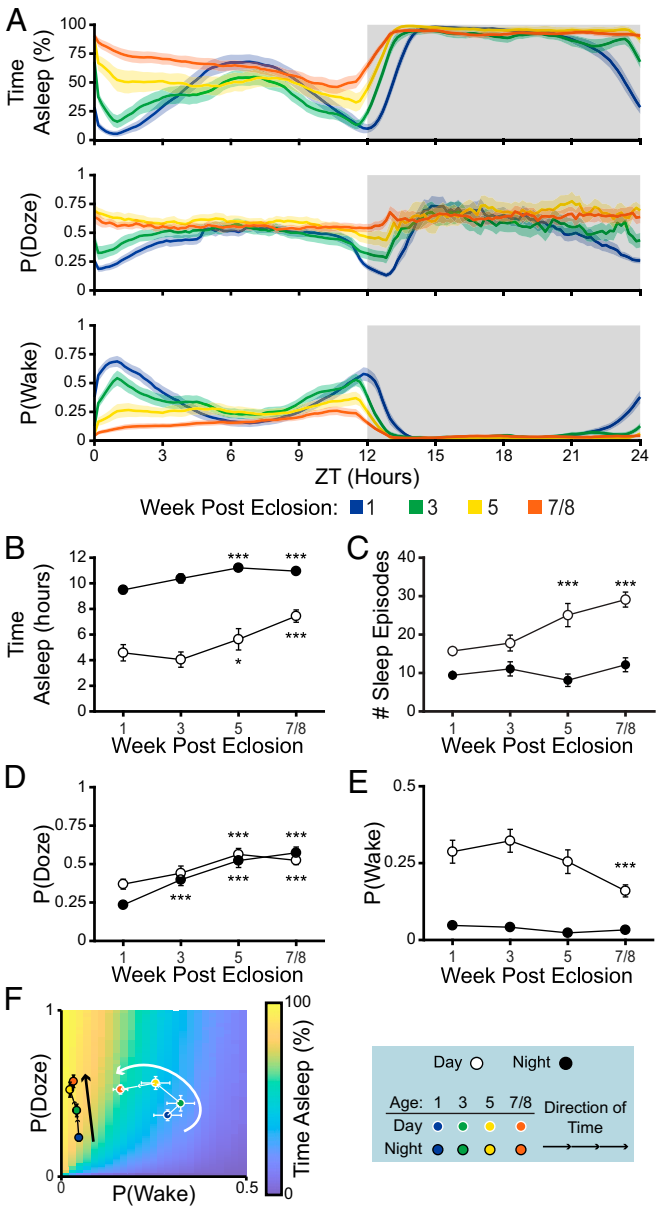

Fig. 6. Changes in sleep due to age are due to both sleep pressure and depth. (*A*) Daily cycle of percentage (%) of Time Asleep, P(Doze), and P(Wake) for wild-type (CS) flies at 1, 3, 5, or 7+ wk post eclosion. (*B–D*) Comparison of time asleep (*B*), number (#) of sleep episodes (*C*), P(Doze) (*D*), and P(Wake) (*E*) across aging during daytime (open circles) and nighttime (filled circles). Error bars are SEM. (*F*) The population means of the aging fly cohorts are overlaid on the in silico-predicted sleep heatmap. Daytime values: white outline; nighttime values: black outline. *n.s.*, no significant difference; $*P < 0.05$; $***P < 0.0005$.

The four-state model is composed of deep sleep, light sleep, early wake, and full wake (Fig. 7*A*). The model definition requires that transitions from wake to sleep must begin in light sleep and that transitions from sleep to wake must begin in early wake (a "sleep inertia"-like property). The permitted hidden state transition probabilities were fitted to the behavior of WT flies in a 12:12 light:dark cycle and per^{01} flies in constant darkness. Despite the substantial differences in sleep phenotype between WT and per^{01} flies, the inferred hidden state transition probabilities and emission probabilities were extremely similar (*SI Appendix*, Table S1), indicating that the existence and

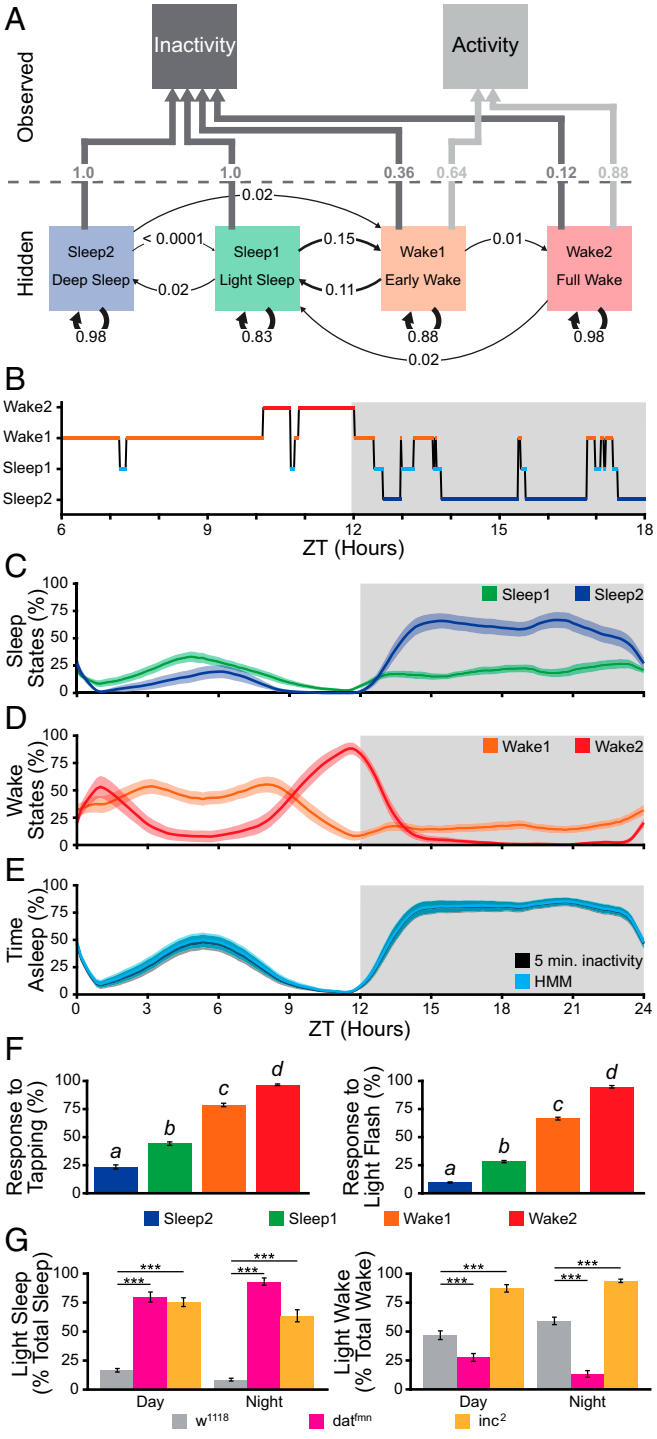

Fig. 7. A four-state Hidden Markov Model. (*A*) The states and state-transition probabilities (per minute) of the HMM. Thickness of the arrows roughly indicates the probability of each state transition; numbers indicate exact probability inferred from *per*^{01} flies in constant darkness. Transitions between states with no line connecting them (e.g., deep sleep and full wake) are not permitted by the model. (*B*) Example of decoded state history of a single WT fly around the time of the light-to-dark transition at ZT 12. Gray area indicates lights-off time. (*C* and *D*) Daily cycle of state probability for the sleep states (*C*) and wake states (*D*) in WT flies (same fly cohort as presented in Fig. 1). (*E*) Daily cycle of total sleep in WT flies measured by HMM decoding and by the 5-min inactivity threshold. (*F*) Percentage (%) of flies in each of the four hidden states that respond to a gentle tap (*Left*) or a brief light flash (*Right*). Means with the different letters are significantly different from one another ($P < 0.0001$; same fly cohorts as presented in Fig. 2 and *SI Appendix*, Fig. S4). (*G*) Percentage (%) of Total Sleep spent in Light Sleep (*Left*) and % Total Wake spent in Light Wake (*Right*) in control (w^{1118}), *fumin* (dat^{fmn}), and *insomniac* (inc^2) flies (same fly cohort as presented in *SI Appendix*, Fig. S7). ***$P < 0.0005$.

properties of these hidden states are robust and both clock and light independent. The fitted HMM can be used to find the posterior probability of each hidden state in a behavioral sequence of an individual animal, thereby decoding its behavior into one of four states (Fig. 7*B*). The average occupancy of each hidden state varies over the daily cycle, with deep sleep occurring predominantly at night and full wake occurring primarily during the morning and evening activity peaks (Fig. 7 *C* and *D*). Interestingly, the total sleep (light and deep) inferred by the four-state HMM is identical to the total sleep as measured using the 5-min threshold (17, 18), even though the sleep definitions are independently derived (Fig. 7*E*).

We tested the relevance of HMM decoding by testing the sensitivity of flies to an arousing stimulus in each hidden state (Fig. 7*F*). Flies have significantly greater arousal probability in light sleep than in deep sleep, and greater arousal probability in full wake than light wake ($P < 0.0001$). Because the emission probabilities of deep and light sleep are both zero, the primary difference between these hidden states is their respective probability of transitioning to wake (*SI Appendix*, Table S1). Likewise, the primary difference between early and full wake is their respective probability to transition to sleep. We hypothesized that the fraction of sleep in deep sleep and the fraction of wake in full wake would be the HMM correlates of P(Wake) and P(Doze), respectively. We tested this hypothesis by examining the sleep mutants *fumin* (14), and *insomniac* (42) (*SI Appendix*, Fig. S7) using the HMM. The % deep sleep and % light wake differ significantly between w^{1118}, *fumin*, and *insomniac* flies ($P < 0.0001$; Fig. 7*G*). In these disparate groups of flies, P(Wake) is correlated with % light sleep ($R = 0.84$, $P < 0.0001$) while P(Doze) is correlated with % light wake ($R = 0.90$, $P < 0.0001$). Overall, the HMM approach recapitulates the results of the P(Wake)- and P(Doze)-based analysis with the benefit of allowing decoding of behavior into discrete categories that may be tied to different circuit configurations or balances between circuits.

Discusssion

Sleep is regulated by a large number of internal and external forces. Competing or interacting switches which are organized hierarchically or into distinct units can allow many factors to be integrated. Understanding the role of a single switch in the system can be difficult if only its effect on the amount of sleep is known. In this paper we address this fundamental problem by measuring and modeling sleep in terms of the probability of activity-state transitions. We define two metrics, P(Wake) and P(Doze), that together can explain the amount of total sleep expressed by individual animals under a variety of conditions. We go on to show, using an HMM, that the numerous wake- and sleep-promoting loci of the fly brain can configure multiple distinct sleep/wake substates that relate directly to P(Doze) and P(Wake) processes. Finally, we demonstrate that fly sleep drives and substates are correlates of underlying biological processes.

Probability of Wake Is a Measure of Sleep Depth. The depth of sleep is clinically important and tied to its restorative power (3). In humans, sleep depth is measured using vital signs, EEG, and behavior, which together provide a holistic view of the process (43). Sleep depth in flies is more difficult to characterize. Total local field potential power in flies is significantly reduced immediately after the initiation of sleep, but does not scale to indicate increased depth of sleep even as the arousal threshold

changes (24, 44). Sleep depth is therefore most commonly measured in flies using arousal threshold in response to an applied sensory stimulus (17, 18, 22–25).

Unfortunately, reliance on sensory arousal thresholds incurs two significant confounds for the experimenter: the regulation of sensory systems by time of day and the disruptive nature of the measurement. Like other animals, the sensory systems of *Drosophila* are regulated by the circadian clock. This has been most robustly demonstrated in the response to light (27, 45, 46) and to odors (28, 47). The major confounding feature of sensory arousal threshold, however, is that it unavoidably disrupts sleep. Rousing the flies is likely to disrupt the deeper-sleep substates found in longer-sleep episodes (24). Repeated rousing may activate homeostatic mechanisms that alter sleep depth (18), and fragmentation of sleep without sleep loss can even trigger sleep rebound (48). Finally, the arousing stimulus may act as a Zeitgeber to the circadian system (49).

In light of these confounds to the sensory arousal threshold, a noninvasive measure of sleep depth would be extremely helpful in understanding the function and regulation of sleep in *Drosophila*. P(Wake) is an attractive alternative measure, and several lines of evidence reinforce its validity as a measure of sleep depth. Most directly, our arousal threshold experiments demonstrate that P(Wake) correlates very significantly with ability to be aroused by either a mechanical or light stimulus (Fig. 2 and *SI Appendix*, Fig. S4). We also find that the arousal-associated molecule dopamine increases P(Wake) in both chronic and acute activation experiments (Fig. 4 and *SI Appendix*, Fig. S7). This is consistent with observations that the rate of spontaneous self-awakening is lower during deeper sleep stages in humans (50). Considering this evidence, we propose that P(Wake) is a behavioral correlate of sleep depth in flies the magnitude of which is closely aligned with dopaminergic tone.

Probability of Doze Is a Measure of Sleep Pressure. After long periods of wake, the desire to sleep also increases. This homeostasis-promoting desire to sleep is described as "sleep pressure," or process S, in the influential Borbély two-factor model of sleep (30). Sleep pressure is difficult to measure directly because it is an internal drive rather than an external behavior. The most common measure of sleep pressure is indirect —a change in the amount of total sleep from baseline, i.e., rebound sleep after deprivation (25). However, this metric is inevitably confounded by sleep depth, which increases in rebound sleep and which we show is the major driver of the amount of sleep across conditions (Figs. 1, 3, and 4). Another common measure of sleep pressure is the latency to sleep after an environmental cue, such as lights turning off (23, 51). Sleep latency is not confounded by sleep depth, but it can only be measured relative to a predefined marker and only once per fly per event, limiting both its temporal resolution and statistical power.

Probability of ceasing activity, P(Doze), is conceptually similar to sleep latency. The primary difference between the two measures is that sleep latency is measured against a discrete external time marker, while P(Doze) is measured using fly-initiated activity, providing a continuous readout. Due to this similarity, we expected that P(Doze) would measure a similar biological process to sleep latency, namely sleep pressure. Empirically, we find that P(Doze) behaves as we would expect a measure of sleep pressure to behave. First, P(Doze) increases precede sleep increases and P(Doze) decreases lag behind sleep as debt is discharged (Fig. 3*C*). Second, P(Doze) is not a major determinant of total sleep in unmanipulated flies, consistent with findings showing that inhibition of the sleep homeostat has only a minimal effect on baseline sleep (52, 53). Third, and perhaps most importantly, we show that P(Doze) has "memory trace" properties: after sleep deprivation it remains elevated until the completion of rebound sleep (Fig. 3).

While the similarities to process S are striking, the daily pattern of P(Doze) does not have the same shape as Borbély's conceptualization (30). Process S is noncircadian and increases steadily during wakefulness, while P(Doze) is fairly flat with troughs during the morning and evening peaks of activity (Fig. 1) (54). This could be due to P(Doze) not being a "pure" sleep pressure signal: P(Doze) is clearly influenced by the clock and by light (Fig. 1), tying P(Doze) to the animals' internal and external states. This is consistent with the idea that the homeostat has a relatively minor role in the specification of sleep drive in unperturbed animals and is engaged only in the case of deviation from the norm. Notably, in our sleep deprivation experiments the trajectory of P(Doze) becomes much more similar to S as sleep debt builds up (Fig. 3*C*). Alternatively, it may be that the two-process model simply does not reflect regulation of sleep pressure in *Drosophila*. Recent evidence suggests that sleep pressure in flies is primarily regulated by the circadian clock rather than by sleep debt (21). The lack of agreement between model and empirical results suggests the need for a revised and more broadly based model of sleep drives.

Counterintuitively for a measure of sleep pressure, P(Doze) is correlated with increased sleep fragmentation (Fig. 5). P(Doze) is the probability of initiating sleep episodes, and since the median sleep episode is shorter than the mean episode in the typical distribution of episode durations for normal animals (55, 56), it follows that increasing P(Doze) will usually result in shorter mean sleep episode duration. The important implication of this finding is that sleep fragmentation is not, on its own, evidence of a wake-promoting process. Our results indicate that fragmented sleep can be the result of decreased sleep depth [i.e., high P(Wake)], increased sleep pressure [i.e., high P(Doze)] or a combination of the two. In line with this, we have recently shown that activation of serotonergic neurons that fragment sleep without changing its total amount primarily increases P(Doze) (48). Biologically, this may make sense. Allowing fragmentation of sleep (which can have advantages under some conditions, e.g., starvation) to be generated by a process untethered to arousal threshold or dopaminergic tone gives the brain more degrees of freedom in determining sleep patterns.

Integration of P(Wake) and P(Doze). Our transition-probability analytical method defines two parameters that can assess the core drives that determine sleep and wake. Importantly, these parameters are only moderately correlated with one another at baseline and are not always affected in concert by perturbations. Some perturbations appear to act primarily on P(Wake) and some primarily on P(Doze). For example, acute increases in dopaminergic tone have strong and consistent effects on P(Wake) and variable effects on P(Doze). In contrast, other perturbations of the system (e.g., aging and mechanical sleep deprivation) alter both P(Doze) and P(Wake). During sleep deprivation, P(Doze) measures sleep need, but decreased P(Wake) is the primary driver of the amount of rebound sleep (Fig. 3), indicating that the two processes interact. These interactions may give additional insight into the privileged roles of some neural circuits in increasing total sleep after sleep deprivation (34) and into the ability of some forms of sleep deprivation to bypass engaging the homeostat (57).

A Hidden Markov Model for *Drosophila* Sleep Substates. P(Wake) and P(Doze) are of only limited utility for classifying flies as being in discrete sleep/wake substates. The P(Wake)/P(Doze)/Sleep landscape (Fig. 1) shows smooth gradients without clear breakpoints or substates. The technical ability to identify and perturb sleep substages in real time has yielded significant insight into the neurophysiology of sleep in mammals (58, 59), so we

developed a tool for classifying fly sleep into hidden states using a HMM. The hidden states decoded by the HMM are distinct in their responses to outside stimuli and internally generated movement in a way that is extremely similar to P(Wake) and P(Doze) (Fig. 7).

Despite their similarities, the conditional probability approach and the HMM have different strengths and weaknesses. Conditional probabilities are naturally scalar, agnostic with regard to underlying biology, and can be estimated from relatively small samples of flies. However, the conditional probabilities are sometimes undefined (*Methods*) and are of limited usefulness in real-time applications. The HMM excels in classifying behavior into distinct hidden states for post hoc analysis or real-time perturbation using the short-time Viterbi algorithm (60). The HMM also requires significant training data if the genetic background or baseline conditions of an experiment preclude reusing a previously trained network model. Importantly, however, we find that the conditional probability and HMM approaches appear to respond to the same underlying drives and are altered in similar manners by experimental perturbations. The complementary strengths of each approach will allow greater flexibility for investigators in experimental design and analysis.

Conclusions

Classifying behavior into discrete units to determine transition probabilities and pathways is an approach that has been applied to many behaviors, including swimming (61), grooming (62), feeding (63), and navigation (64, 65). Use of Hidden Markov Modeling to decode coherent brain or behavioral states has also been widely applied (66–70). In this report, we utilize locomotor data to measure the probability that an animal transitions between sleep and wake states and build an HMM that allows us to identify multiple distinct wake and sleep states. As our understanding of sleep grows, it has become clear that two individuals displaying the same amount of sleep may have arrived at that amount on very different paths. The ability to characterize a sleep set point in terms of the animal's underlying arousal level and sleep drive will help tease apart the complexities of the circuits that specify sleep under different environmental and internal conditions.

Methods

Animals. Flies were raised on cornmeal–dextrose–yeast food in a 25 °C incubator. The incubator maintained a 12 h:12 h light:dark cycle. Transgenic flies used were the following: per^{01}(CS)—a gift of Michael Rosbash (Brandeis University, Waltham, MA) —w^{1118} and w^{1118}; dat^{fmn}—gift of Amita Sehgal (University of Pennsylvania, Philadelphia, PA) —PBac{WH}inc^{f00285}, w^{1118} (inc^{2}; BDSC # 18307), *TH-Gal4* (BDSC # 8848), and *UAS-dTrpA* (37).

Sleep Data Collection. Data were collected using the DAM system and Flybox as previously reported (19, 71). Unless otherwise specified, experiments were carried out at 25 °C with a 12 h:12 h light:dark cycle. The light-driven arousal threshold in the DAM system was measured in a dimly lit incubator by delivering 3-s pulses of red light. The mechanical arousal threshold in the Flybox was measured by applying a single tap to the side of the 96-well plate using a solenoid.

Generation of In Silico Data. Simulation data were generated by custom programs written in Matlab (MathWorks, Natick, MA). The simulation was initialized in a random state with equal probability of wake and sleep. At each subsequent time step, the simulator checked the current state of the fly, generated a random number between 0 and 1, and compared the value with P(Wake) or P(Doze) to determine if the in silico fly woke or dozed, as appropriate.

Data Analysis. DAM system, Flybox, and in silico data were analyzed with a common set of modular programs written in Matlab. P(Wake) was calculated as follows: 1) Every bin of inactivity was counted except the last one: this quantity was the denominator, the total number of state transitions from inactivity; 2) For every bin of inactivity, the number of times the fly was active were counted in the subsequent bin: this quantity was the numerator, the total number of state transitions from inactive to active; 3) The total of state transitions from inactive to active were divided by the total state transitions from inactive. If there were no bins where the fly did not move (i.e., denominator is zero), the transition probability was considered undefined. P(Doze) was calculated identically, but with activity and inactivity reversed. The choice of using 1-min activity bins instead of 5-min sleep/wake as the basis for the analysis was made after considering both methods (*SI Appendix*, Fig. S8).

Statistical Analysis. Statistical analysis was performed using the Matlab statistics toolbox. Fitting of HMMs and decoding of hidden states were performed using the Matlab Statistics and Machine Learning Toolkit.

Data Sharing and Code. Statistical treatments and information are provided for each figure in *SI Appendix, Supplemental Statistical Tables*. The MATLAB scripts for analysis of P(Wake)/P(Doze) and for HMM functions have been deposited in GitHub and can be accessed at https://github.com/Griffith-Lab/Fly_Sleep_Probability.

ACKNOWLEDGMENTS. This work was funded by NIH Grants R01 MH067284 (to L.C.G.) and F32 NS098624 (to T.D.W.). We thank Dr. Jané Kondev and the students in the Brandeis Quantitative Biology Research Community who assisted in collecting preliminary data and Dr. Michael Rosbash and the Brandeis Science Communication Lab for helpful comments on this manuscript.

1. E. N. Brown, R. Lydic, N. D. Schiff, General anesthesia, sleep, and coma. *N. Engl. J. Med.* **363**, 2638–2650 (2010).
2. C. von Economo, Sleep as a problem of localization. *J. Nerv. Ment. Dis.* **71**, 249–259 (1930).
3. T. E. Scammell, E. Arrigoni, J. O. Lipton, Neural circuitry of wakefulness and sleep. *Neuron* **93**, 747–765 (2017).
4. J. Tomita, G. Ban, K. Kume, Genes and neural circuits for sleep of the fruit fly. *Neurosci. Res.* **118**, 82–91 (2017).
5. M. E. Yurgel, P. Masek, J. DiAngelo, A. C. Keene, Genetic dissection of sleep-metabolism interactions in the fruit fly. *J. Comp. Physiol. A Neuroethol. Sens. Neural Behav. Physiol.* **201**, 869–877 (2015).
6. D. R. Nässel, M. Zandawala, Recent advances in neuropeptide signaling in Drosophila, from genes to physiology and behavior. *Prog. Neurobiol.* **179**, 101607 (2019).
7. L. Barateau, R. Lopez, J. A. M. Franchi, Y. Dauvilliers, Hypersomnolence, hypersomnia, and mood disorders. *Curr. Psychiatry Rep.* **19**, 13 (2017).
8. A. Kales, J. D. Kales, Sleep disorders. Recent findings in the diagnosis and treatment of disturbed sleep. *N. Engl. J. Med.* **290**, 487–499 (1974).
9. M. T. Bianchi *et al*., Probabilistic sleep architecture models in patients with and without sleep apnea. *J. Sleep Res.* **21**, 330–341 (2012).
10. L. Perez-Atencio, N. Garcia-Aracil, E. Fernandez, L. C. Barrio, J. A. Barios, A four-state Markov model of sleep-wakefulness dynamics along light/dark cycle in mice. *PLoS One* **13**, e0189931 (2018).
11. R. Stephenson, A. M. Caron, S. Famina, Significance of the zero sum principle for circadian, homeostatic and allostatic regulation of sleep-wake state in the rat. *Physiol. Behav.* **167**, 35–48 (2016).
12. M. C. Yang, C. J. Hursch, The use of a semi-Markov model for describing sleep patterns. *Biometrics* **29**, 667–676 (1973).
13. R. Andretic, B. van Swinderen, R. J. Greenspan, Dopaminergic modulation of arousal in Drosophila. *Curr. Biol.* **15**, 1165–1175 (2005).
14. K. Kume, S. Kume, S. K. Park, J. Hirsh, F. R. Jackson, Dopamine is a regulator of arousal in the fruit fly. *J. Neurosci.* **25**, 7377–7384 (2005).
15. K. Koh, J. M. Evans, J. C. Hendricks, A. Sehgal, A Drosophila model for age-associated changes in sleep:wake cycles. *Proc. Natl. Acad. Sci. U.S.A.* **103**, 13843–13847 (2006).
16. J. Vienne, R. Spann, F. Guo, M. Rosbash, Age-related reduction of recovery sleep and arousal threshold in Drosophila. *Sleep (Basel)* **39**, 1613–1624 (2016).
17. P. J. Shaw, C. Cirelli, R. J. Greenspan, G. Tononi, Correlates of sleep and waking in Drosophila melanogaster. *Science* **287**, 1834–1837 (2000).
18. J. C. Hendricks *et al*., Rest in Drosophila is a sleep-like state. *Neuron* **25**, 129–138 (2000).
19. F. Guo *et al*., Circadian neuron feedback controls the Drosophila sleep: Activity profile. *Nature* **536**, 292–297 (2016).
20. S. M. Buchanan, J. S. Kain, B. L. de Bivort, Neuronal control of locomotor handedness in *Drosophila*. *Proc. Natl. Acad. Sci. U.S.A.* **112**, 6700–6705 (2015).
21. Q. Geissmann, E. J. Beckwith, G. F. Gilestro, Most sleep does not serve a vital function: Evidence from *Drosophila melanogaster*. *Sci. Adv.* **5**, eaau9253 (2019).
22. F. Guo, W. Yi, M. Zhou, A. Guo, Go signaling in mushroom bodies regulates sleep in Drosophila. *Sleep (Basel)* **34**, 273–281 (2011).
23. N. J. Linford, T. P. Chan, S. D. Pletcher, Re-patterning sleep architecture in Drosophila through gustatory perception and nutritional quality. *PLoS Genet.* **8**, e1002668 (2012).

24. B. van Alphen, M. H. W. Yap, L. Kirszenblat, B. Kottler, B. van Swinderen, A dynamic deep sleep stage in Drosophila. *J. Neurosci.* **33**, 6917–6927 (2013).
25. R. Huber *et al*., Sleep homeostasis in Drosophila melanogaster. *Sleep* **27**, 628–639 (2004).
26. K. M. Parisky, J. L. Agosto Rivera, N. C. Donelson, S. Kotecha, L. C. Griffith, Reorganization of sleep by temperature in Drosophila requires light, the homeostat, and the circadian clock. *Curr. Biol.* **26**, 882–892 (2016).
27. D. M. Chen, J. S. Christianson, R. J. Sapp, W. S. Stark, Visual receptor cycle in normal and period mutant Drosophila: Microspectrophotometry, electrophysiology, and ultrastructural morphometry. *Vis. Neurosci.* **9**, 125–135 (1992).
28. B. Krishnan, S. E. Dryer, P. E. Hardin, Circadian rhythms in olfactory responses of Drosophila melanogaster. *Nature* **400**, 375–378 (1999).
29. P. M. Fuller, J. J. Gooley, C. B. Saper, Neurobiology of the sleep-wake cycle: Sleep architecture, circadian regulation, and regulatory feedback. *J. Biol. Rhythms* **21**, 482–493 (2006).
30. A. A. Borbély, A two process model of sleep regulation. *Hum. Neurobiol.* **1**, 195–204 (1982).
31. D. J. Cavanaugh, A. S. Vigderman, T. Dean, D. S. Garbe, A. Sehgal, The *Drosophila* circadian clock gates sleep through time-of-day dependent modulation of sleep-promoting neurons. *Sleep (Basel)* **39**, 345–356 (2016).
32. J. Cohen, Statistical power analysis. *Curr. Dir. Psychol. Sci.* **1**, 98–101 (1992).
33. C. Helfrich-Förster, Sleep in insects. *Annu. Rev. Entomol.* **63**, 69–86 (2018).
34. G. Seidner *et al*., Identification of neurons with a privileged role in sleep homeostasis in Drosophila melanogaster. *Curr. Biol.* **25**, 2928–2938 (2015).
35. Y. Shang *et al*., Imaging analysis of clock neurons reveals light buffers the wake-promoting effect of dopamine. *Nat. Neurosci.* **14**, 889–895 (2011).
36. T. Ueno *et al*., Identification of a dopamine pathway that regulates sleep and arousal in Drosophila. *Nat. Neurosci.* **15**, 1516–1523 (2012).
37. F. N. Hamada *et al*., An internal thermal sensor controlling temperature preference in Drosophila. *Nature* **454**, 217–220 (2008).
38. M. H. Silber *et al*., The visual scoring of sleep in adults. *J. Clin. Sleep Med.* **3**, 121–131 (2007).
39. C. Iber, S. Ancoli-Israel, A. L. Chesson, S. Quan, *The AASM Manual for the Scoring of Sleep and Associated Events: Rules, Terminology and Technical Specifications*. (American Academy of Sleep Medicine, 2007).
40. T. P. Gilmour, J. Fang, Z. Guan, T. Subramanian, Manual rat sleep classification in principal component space. *Neurosci. Lett.* **469**, 97–101 (2010).
41. M. M. Lacroix *et al*., Improved sleep scoring in mice reveals human-like stages. bioRxiv 10.1101/489005 (2018).
42. N. Stavropoulos, M. W. Young, Insomniac and Cullin-3 regulate sleep and wakefulness in Drosophila. *Neuron* **72**, 964–976 (2011).
43. M. H. Bonnet *et al*., The scoring of arousal in sleep: Reliability, validity, and alternatives. *J. Clin. Sleep Med.* **3**, 133–145 (2007).
44. M. H. W. Yap *et al*., Oscillatory brain activity in spontaneous and induced sleep stages in flies. *Nat. Commun.* **8**, 1815 (2017).
45. L. S. Baik, Y. Recinos, J. A. Chevez, T. C. Holmes, Circadian modulation of light-evoked avoidance/attraction behavior in Drosophila. *PLoS One* **13**, e0201927 (2018).
46. O. M. Nippe, A. R. Wade, C. J. H. Elliott, S. Chawla, Circadian rhythms in visual responsiveness in the behaviorally arrhythmic Drosophila clock mutant Clk^{Jrk}. *J. Biol. Rhythms* **32**, 583–592 (2017).
47. X. Zhou, C. Yuan, A. Guo, Drosophila olfactory response rhythms require clock genes but not pigment dispersing factor or lateral neurons. *J. Biol. Rhythms* **20**, 237–244 (2005).
48. C. Liu *et al*., A serotonin-modulated circuit controls sleep architecture to regulate cognitive function independent of total sleep in Drosophila. *Curr. Biol.* **29**, 3635–3646.e5 (2019).
49. C. Lee, V. Parikh, T. Itsukaichi, K. Bae, I. Edery, Resetting the Drosophila clock by photic regulation of PER and a PER-TIM complex. *Science* **271**, 1740–1744 (1996).
50. H. Zepelin, REM sleep and the timing of self-awakenings. *Bull. Psychon. Soc.* **24**, 254–256 (1986).
51. R. Andretic, P. J. Shaw, Essentials of sleep recordings in Drosophila: Moving beyond sleep time. *Methods Enzymol.* **393**, 759–772 (2005).
52. C. Dubowy *et al*., Genetic dissociation of daily sleep and sleep following thermogenetic sleep deprivation in *Drosophila*. *Sleep (Basel)* **39**, 1083–1095 (2016).
53. S. Liu, Q. Liu, M. Tabuchi, M. N. Wu, Sleep drive is encoded by neural plastic changes in a dedicated circuit. *Cell* **165**, 1347–1360 (2016).
54. D. Rieger, O. T. Shafer, K. Tomioka, C. Helfrich-Förster, Functional analysis of circadian pacemaker neurons in Drosophila melanogaster. *J. Neurosci.* **26**, 2531–2543 (2006).
55. J. M. Diamond, Goodness of fit to a mathematical model for Drosophila sleep behavior is reduced in hyposomnolent mutants. *PeerJ.* **4**, e1533 (2016).
56. T. Ueno, N. Masuda, S. Kume, K. Kume, Dopamine modulates the rest period length without perturbation of its power law distribution in Drosophila melanogaster. *PLoS One* **7**, e32007 (2012).
57. E. J. Beckwith, Q. Geissmann, A. S. French, G. F. Gilestro, Regulation of sleep homeostasis by sexual arousal. *eLife* **6**, e27445 (2017).
58. S. J. Casey *et al*., Slow wave and REM sleep deprivation effects on explicit and implicit memory during sleep. *Neuropsychology* **30**, 931–945 (2016).
59. Y. S. Ju *et al*., Slow wave sleep disruption increases cerebrospinal fluid amyloid-β levels. *Brain* **140**, 2104–2111 (2017).
60. J. Bloit, X. Rodet, "Short-time Viterbi for online HMM decoding: Evaluation on a real-time phone recognition task" in *2008 IEEE International Conference on Acoustics, Speech and Signal Processing*, (IEEE, 2008), pp. 2121–2124.
61. A. O. Willows, G. Hoyle, Neuronal network triggering a fixed action pattern. *Science* **166**, 1549–1551 (1969).
62. K. C. Berridge, J. C. Fentress, H. Parr, Natural syntax rules control action sequence of rats. *Behav. Brain Res.* **23**, 59–68 (1987).
63. M. Martaresche, C. Le Fur, M. Magnusson, J. M. Faure, M. Picard, Time structure of behavioral patterns related to feed pecking in chicks. *Physiol. Behav.* **70**, 443–451 (2000).
64. S. Kato *et al*., Global brain dynamics embed the motor command sequence of Caenorhabditis elegans. *Cell* **163**, 656–669 (2015).
65. L. Hernandez-Nunez *et al*., Reverse-correlation analysis of navigation dynamics in Drosophila larva using optogenetics. *eLife* **4**, e06225 (2015).
66. S.-T. Pan, C.-E. Kuo, J.-H. Zeng, S.-F. Liang, A transition-constrained discrete hidden Markov model for automatic sleep staging. *Biomed. Eng. Online* **11**, 52 (2012).
67. D. Vidaurre, S. M. Smith, M. W. Woolrich, Brain network dynamics are hierarchically organized in time. *Proc. Natl. Acad. Sci. U.S.A.* **114**, 12827–12832 (2017).
68. A. B. A. Stevner *et al*., Discovery of key whole-brain transitions and dynamics during human wakefulness and non-REM sleep. *Nat. Commun.* **10**, 1035 (2019).
69. N. J. Williams, I. Daly, S. J. Nasuto, Markov model-based method to analyse time-varying networks in EEG task-related data. *Front. Comput. Neurosci.* **12**, 76 (2018).
70. B. F. Sadacca *et al*., The behavioral relevance of cortical neural ensemble responses emerges suddenly. *J. Neurosci.* **36**, 655–669 (2016).
71. P. R. Goodwin *et al*., MicroRNAs regulate sleep and sleep homeostasis in Drosophila. *Cell Rep.* **23**, 3776–3786 (2018).